

Multiorbital analysis of the effects of uniaxial and hydrostatic pressure on T_c in the single-layered cuprate superconductors

Hirofumi Sakakibara¹, Katsuhiko Suzuki^{1,6}, Hidetomo Usui², Kazuhiko Kuroki^{1,6}, Ryotaro Arita^{3,6,7}, Douglas J. Scalapino⁵, and Hideo Aoki^{4,6}

¹*Department of Engineering Science, The University of Electro-Communications, Chofu, Tokyo 182-8585, Japan*

²*Department of Applied Physics and Chemistry, The University of Electro-Communications, Chofu, Tokyo 182-8585, Japan*

³*Department of Applied Physics, The University of Tokyo, Hongo, Tokyo 113-8656, Japan*

⁴*Department of Physics, The University of Tokyo, Hongo, Tokyo 113-0033, Japan*

⁵*Physics Department, University of California, Santa Barbara, California 93106-9530, USA*

⁶*JST, TRIP, Sanbancho, Chiyoda, Tokyo 102-0075, Japan and*

⁷*JST, PRESTO, Kawaguchi, Saitama 332-0012, Japan*

(Dated: November 8, 2018)

The origin of uniaxial and hydrostatic pressure effects on T_c in the single-layered cuprate superconductors is theoretically explored. A two-orbital model, derived from first principles and analyzed with the fluctuation exchange approximation gives axial-dependent pressure coefficients, $\partial T_c / \partial P_a > 0$, $\partial T_c / \partial P_c < 0$, with a hydrostatic response $\partial T_c / \partial P > 0$ for both La214 and Hg1201 cuprates, in qualitative agreement with experiments. Physically, this is shown to come from a unified picture in which higher T_c is achieved with an “orbital distillation”, namely, the less the $d_{x^2-y^2}$ main band is hybridized with the d_{z^2} and 4s orbitals higher the T_c . Some implications for obtaining higher T_c materials are discussed.

PACS numbers: 74.20.-z, 74.62.Bf, 74.72.-h

I. INTRODUCTION

In the physics of high- T_c cuprates, optimizing their T_c remains a fundamental yet still open problem. Empirically, important parameters that control T_c have been identified for the cuprates, i.e., chemical composition, structural parameters, the number of layers, etc, besides the doping concentration. For the structural parameters specifically, several key quantities have been suggested: the bond length between copper and in-plane oxygen (l , defined in Fig.1)^{1,2}, and the Cu-apical oxygen distance (h_O)³⁻¹¹.

Now, the pressure effect is exceptionally valuable as an *in situ* way to probe the structure-dependence of T_c . Regarding this, two general observations have been made for the cuprates: (i) T_c tends to be enhanced under hydrostatic pressure, while (ii) uniaxial pressures produce anisotropic responses of T_c . More precisely, (i) T_c has been shown to monotonically increase for pressure < 30 GPa^{12,13}. As for (ii), an a -axis compression generally raises T_c ($\partial T_c / \partial P_a > 0$), while c -axis compression has an opposite effect ($\partial T_c / \partial P_c < 0$)¹⁴⁻¹⁶. Moreover, the magnitude of the pressure coefficient becomes smaller for materials having higher T_c 's, as summarized in Fig.3 of ref.¹⁴. The purpose of the present study is to theoretically reveal the origin of these general trends, focusing on the single-layered cuprates for clarity, and to shed light on a possibility of further optimizing T_c .

Conventionally, the theoretical model primarily used for the cuprates is a one-band Hubbard model based on the $d_{x^2-y^2}$ orbital (or sometimes Cu- $3d_{x^2-y^2} + O-2p_\sigma$ orbital). Recently, we have shown^{10,11} that the d_{z^2} orbital component strongly mixes into the states on the Fermi surface in the relatively low- T_c cuprates such as

La₂CuO₄ (La214)¹⁷⁻¹⁹, where the hybridization works destructively against d -wave superconductivity. While there have been some theoretical studies in the literature focusing on the role of the d_{z^2} orbital^{7,8,20-23}, Refs.^{10,11} conclude that larger the level offset ΔE between the $d_{x^2-y^2}$ and d_{z^2} Wannier orbitals, higher the T_c , where ΔE is governed by the apical-oxygen height and the inter-layer distance. One might then presume that the effects of uniaxial pressures can simply be captured in terms of the pressure-dependence of ΔE affected by the crystal field. However, we reveal in the present work that the physics is not so simple. We find that, while the variation of T_c under pressure is indeed affected by ΔE , especially in the relatively low- T_c cuprates, the large ΔE values in higher- T_c cuprates such as HgBa₂CuO₄ (Hg1201) make their relevance to the T_c variation smaller. We shall show that we have to turn our attention rather to the Cu4s level, which is raised with pressure, resulting in a less rounded (i.e., better nested) Fermi surface. This, along with the increase in the band width, is shown to cause a higher T_c under pressure. These results can be unified into a picture in which higher T_c can be achieved by the “distillation” of the main (i.e., $d_{x^2-y^2}$) band, namely, the smaller the hybridization of other orbital components the better.

II. FORMULATION

A. Construction of the two-orbital model

Our theoretical procedure is as follows. We first determine the lattice structure under uniaxial and hydrostatic pressures from a first-principles band calculation

with the Wien2k package²⁴. From the band structure, we construct the maximally-localized Wannier orbitals^{25,26} to obtain the hopping integrals for a two-orbital tight-binding model that takes into account both the $d_{x^2-y^2}$ and the d_{z^2} Wannier orbitals explicitly¹⁰.

B. Many body analysis

In this two-orbital model, we consider the onsite intra- and inter-orbital electron-electron repulsive interactions, which are given, in the standard notation, as

$$\begin{aligned}
H = & \sum_i \sum_\mu \sum_\sigma \varepsilon_\mu n_{i\mu\sigma} + \sum_{ij} \sum_{\mu\nu} \sum_\sigma t_{ij}^{\mu\nu} c_{i\mu\sigma}^\dagger c_{j\nu\sigma} \\
& + \sum_i \left(U \sum_\mu n_{i\mu\uparrow} n_{i\mu\downarrow} + U' \sum_{\mu>\nu} \sum_{\sigma,\sigma'} n_{i\mu\sigma} n_{i\nu\sigma'} \right. \\
& - \frac{J}{2} \sum_{\mu\neq\nu} \sum_{\sigma,\sigma'} c_{i\mu\sigma}^\dagger c_{i\mu\sigma'} c_{i\nu\sigma'}^\dagger c_{i\nu\sigma} \\
& \left. + J' \sum_{\mu\neq\nu} c_{i\mu\uparrow}^\dagger c_{i\mu\downarrow}^\dagger c_{i\nu\downarrow} c_{i\nu\uparrow} \right), \quad (1)
\end{aligned}$$

where i, j denote the sites while μ, ν the two orbitals, the electron-electron interactions comprise the intraorbital repulsion U , interorbital repulsion U' , and the Hund's coupling J (= pair-hopping interaction J'). Here we take $U = 3.0$ eV, $U' = 2.4$ eV, and $J = 0.3$ eV². These values conform to widely accepted, first-principles estimations for the cuprates that U is 7-10 t (with $t \simeq 0.45$ eV), while $J, J' \simeq 0.1U$. Here we also observe the orbital SU(2) requirement, $U' = U - 2J$.

To study the superconductivity in this multi-orbital Hubbard model, we apply the fluctuation exchange approximation (FLEX)²⁷⁻²⁹. In FLEX, we start with Dyson equation to obtain the renormalized Green's function, which is, in the multi-orbital case, a matrix in the orbital representation as $G_{l_1 l_2}$, where l_1 and l_2 are orbital indices. The bubble and ladder diagrams constructed from the renormalized Green's function are then summed to obtain the spin and charge susceptibilities,

$$\hat{\chi}_s(q) = \frac{\hat{\chi}^0(q)}{1 - \hat{S} \hat{\chi}^0(q)}, \quad (2)$$

$$\hat{\chi}_c(q) = \frac{\hat{\chi}^0(q)}{1 + \hat{C} \hat{\chi}^0(q)}, \quad (3)$$

where $q \equiv (\mathbf{q}, i\omega_n)$ with wave vector \mathbf{q} and with Matsubara frequency $i\omega_n \equiv (2n + 1)\pi k_B T$, and the irreducible susceptibility is

$$\chi_{l_1, l_2, l_3, l_4}^0(q) = \sum_q G_{l_1 l_3}(k + q) G_{l_4 l_2}(k), \quad (4)$$

with the interaction matrices

$$S_{l_1 l_2, l_3 l_4} = \begin{cases} U, & l_1 = l_2 = l_3 = l_4 \\ U', & l_1 = l_3 \neq l_2 = l_4 \\ J, & l_1 = l_2 \neq l_3 = l_4 \\ J', & l_1 = l_4 \neq l_2 = l_3, \end{cases} \quad (5)$$

$$C_{l_1 l_2, l_3 l_4} = \begin{cases} U & l_1 = l_2 = l_3 = l_4 \\ -U' + J & l_1 = l_3 \neq l_2 = l_4 \\ 2U' - J, & l_1 = l_2 \neq l_3 = l_4 \\ J' & l_1 = l_4 \neq l_2 = l_3. \end{cases} \quad (6)$$

With these susceptibilities, the fluctuation-mediated effective interactions are obtained, which are used to calculate the self-energy. Then the renormalized Green's functions are determined self-consistently from Dyson equation. The Green's functions and the susceptibilities are used to obtain the spin-singlet pairing interaction in the form

$$\hat{V}^s(q) = \frac{3}{2} \hat{S} \hat{\chi}_s(q) \hat{S} - \frac{1}{2} \hat{C} \hat{\chi}_c(q) \hat{C} + \frac{1}{2} (\hat{S} + \hat{C}), \quad (7)$$

and this is used in the linearized Eliashberg equation,

$$\begin{aligned}
\lambda \Delta_{l'l'}(k) = & -\frac{T}{N} \sum_q \sum_{l_1 l_2 l_3 l_4} V_{l_1 l_2 l''}(q) \\
& \times G_{l_1 l_3}(k - q) \Delta_{l_3 l_4}(k - q) G_{l_2 l_4}(q - k). \quad (8)
\end{aligned}$$

The superconducting transition temperature, T_c , corresponds to the temperature at which the maximum eigenvalue λ of the Eliashberg equation reaches unity, so that λ at a fixed temperature can be used as a measure for T_c . T_c of the Hg cuprate is experimentally about three times higher than in La cuprate³⁰, so we calculate λ by putting $T = 0.01$ eV for La and $T = 0.03$ eV for Hg for a clearer comparison. As we shall see, the eigenvalues discussed in the present study are away from unity (i.e., the temperature is higher than T_c) due to the limitation in the number of Matsubara frequencies and the k -point meshes. Therefore, for the La cuprate in particular, we restrict ourselves to qualitative argument for the T_c variation under pressure. For the Hg cuprate, on the other hand, we can go down to lower temperatures ($T \sim 0.01$) where the eigenvalue approaches unity, and we have checked that the conclusions drawn from the $T = 0.03$ calculation hold also for $T \sim 0.01$. Moreover, we estimate dT_c/dP for Hg with the $T \sim 0.01$ results, as will be discussed in the final part of the paper. We fix the total band filling (number of electrons/site) at $n = 2.85$, for which the filling of the main band amounts to 0.85 (15 % hole doping). We take a $32 \times 32 \times 4$ k -point meshes for the three-dimensional lattice with 1024 Matsubara frequencies.

TABLE I: Structural and electronic parameters obtained from the first-principles(th) and experiments(exp) in ref^{32,33}.

	La(exp)	La(th)	Hg(exp)	Hg(th)
a_0 [Å]	3.78	3.76	3.88	3.84
c_0 [Å]	13.2	13.1	9.51	9.58
h_O [Å]	2.42	2.41	2.78	2.81
$h_{La,Ba}$ [Å]	1.85	1.81	1.92	1.88
V_0 [Å ³]	189	184	143	141
ΔE [eV]	0.857	0.861	2.16	2.305
$r_{x^2-y^2}$	0.363	0.357	0.419	0.411
W [eV]	4.14	4.23	4.06	4.19

III. CALCULATION RESULTS: UNIAXIAL PRESSURE

A. Crystal structure under pressure

Let us begin with the case of uniaxial pressure. We first vary the lattice constants and calculate the total energy E_{tot} . This is fit by the standard Burch-Marnaghan equation³¹ to determine the most stable structure with a unit cell volume $V = V_0$, the a -axis lattice constant $a = a_0$, and the c -axis $c = c_0$. For simplicity, we retain the tetragonal symmetry throughout, i.e., $b = a$ (so that the a -compression is actually biaxial). We show in Table I the lattice parameters, a_0 , c_0 , h_O , $h_{La,Ba}$ (La or Ba height measured from CuO_2 plane) and V_0 , obtained for the La and Hg cuprates. The results are in good agreement with experimental values for the optimally doped compounds^{32,33}. We then relax the structure perpendicular to the compression direction, namely, we allow the lattice constant in that direction to relax to obtain the

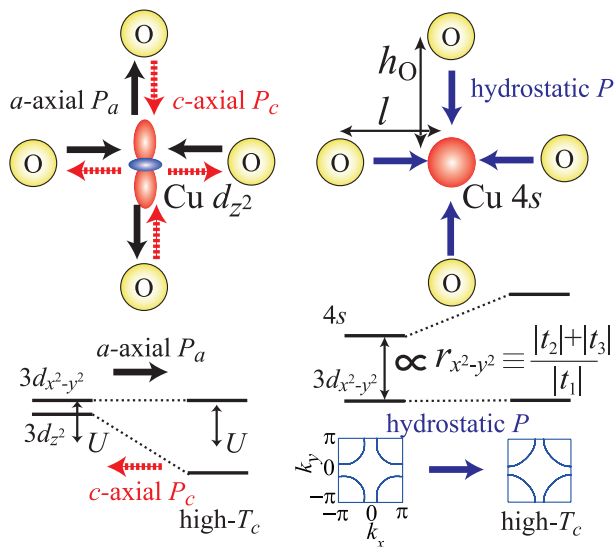


FIG. 1: Bottom left: schematic variation of the d_{z^2} orbital level with respect to that for $d_{x^2-y^2}$ under uniaxial pressure (top left inset). Bottom right: the shift of Cu $4s$ level under hydrostatic pressure and its effect on the Fermi surface.

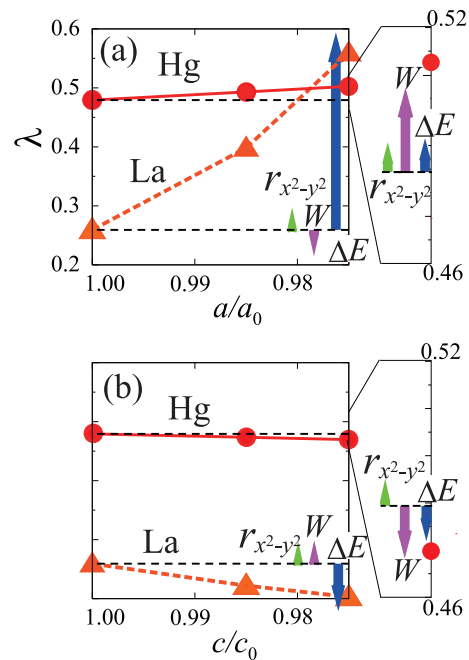


FIG. 2: For uniaxial compressions the eigenvalue λ of the Eliashberg equation is plotted against a/a_0 (a) or c/c_0 (b). Triangles (circles) indicate the result for the La (Hg) cuprates. Arrows depict the contributions (see text) to the λ variation from ΔE , W , and $r_{x^2-y^2}$, respectively, at $a/a_0, c/c_0 = 0.975$. Lines are guide for the eye, with the dashed horizontal ones indicating the original values.

value that gives the lowest energy.

Figure 2 plots the eigenvalue of the Eliashberg equation λ against the lattice compression a/a_0 and c/c_0 for each compound. The result shows that (i) in both compounds λ increases as a/a_0 is reduced, while decreases as c/c_0 is reduced, and (ii) the absolute value of the variations of λ is larger in La than in Hg. These features are in qualitative agreement with the experimental observations summarized in Fig.3 of ref.¹⁴, which shows $\partial T_c / \partial P_a > 0$ and $\partial T_c / \partial P_c < 0$ for both materials, with larger $|\partial T_c / \partial P_i|$ in La than in Hg^{14,15}. To be more precise, while the compressibility in the a direction is nearly the same between the two materials, that in the c direction is about three times larger in Hg than in La^{34,35} ($dc/dP_c|_{\text{Hg}} \simeq 3dc/dP_c|_{\text{La}}$), but even if we take this into account, we find that $\partial \lambda / \partial P_c$ is still larger for La than for Hg in our calculation.

B. Contribution from the d_{z^2} orbital: ΔE

Now we want to pinpoint the origin of this T_c variation against uniaxial pressures. In both materials, $\Delta E \equiv E_{d_{x^2-y^2}} - E_{d_{z^2}}$ increases as a/a_0 is reduced, while it decreases when c/c_0 is reduced. This is natural, since the a (c) reduction pushes the in-plane (out-of-plane) ligands toward Cu, resulting in a larger (smaller) crystal-field

splitting and hence larger (smaller) ΔE^{11} , as schematically depicted in Fig.1. One might then expect that this alone is the origin of the T_c variation, since ΔE and T_c are positively correlated¹⁰. To see if this is indeed the case, we have considered a case where we increase ΔE alone to its value at $a/a_0 = 0.975$ or $c/c_0 = 0.975$, and obtain λ with FLEX. The results are indicated in Fig.2 with arrows labeled as “ ΔE ”. In La, the resulting λ is very close to those obtained for the actual compression, which implies that the main origin for λ variation under uniaxial pressure comes from ΔE . By contrast, for Hg, the ΔE contribution is too small to account for the actual λ variance (see the blowups in Fig.2).

C. Contribution from the 4s orbital: $r_{x^2-y^2}$

The reason for this is that in Hg, ΔE is $\simeq 2.5$ times larger than in La (table I), so that the effect of the d_{z^2} orbital is tiny, while the contribution to the T_c variation coming from other changes in the electronic structure become comparable with that from ΔE . In particular, we focus on the change in the energy difference ΔE_s between Cu4s and $Cu d_{x^2-y^2}$ orbitals. In fact, it has been shown that the Cu4s orbital, which is implicitly included in the $d_{x^2-y^2}$ Wannier orbital in the present scheme, affects the second (t_2) and third (t_3) neighbor hoppings^{4,6,10,11}. Note that the 4s orbital can be integrated out (implicitly included in the Wannier orbitals) prior to the many-body analysis, since the 4s orbital sits in energy well away from the Fermi level in contrast to the d_{z^2} orbital (Fig.1)^{10,11}. Smaller ΔE_s results in larger $r_{x^2-y^2} \equiv (|t_2| + |t_3|)/|t_1|$ within the $d_{x^2-y^2}$ orbital sector, resulting in a more rounded Fermi surface, which degrades d -wave superconductivity^{10,36-38}.

To show how the roundness varies with ΔE_s , we consider a three-orbital model which explicitly includes the Cu 4s Wannier orbitals for the Hg cuprate^{10,11}, and show in Fig.3 the Fermi surface for various values of $\Delta E_s = E_{Cu4s} - E_{Cu3d_{x^2-y^2}}$. We stress here that, while larger ΔE and larger $r_{x^2-y^2}$ (or smaller ΔE_s) both give more rounded Fermi surface, their effects on T_c are opposite. Under pressure, ΔE_s is enhanced, which in turn reduces $r_{x^2-y^2}$. In Fig.2, we show the effect of hypothetically reducing $r_{x^2-y^2}$ down to its values at $a/a_0 = 0.975$ or $c/c_0 = 0.975$. While the effect of $r_{x^2-y^2}$ is much smaller than that of ΔE in La, the two effects are found to be comparable in Hg.

D. Contribution from the band width: W

In addition to ΔE and $r_{x^2-y^2}$, the band width W (the energy difference between $\mathbf{k} = (0,0)$ and (π, π)) of the main band is also altered by pressure. In La the change in λ due to the modification of W is small compared to that arising from ΔE , but in Hg the W contribution is comparable with those from ΔE and $r_{x^2-y^2}$, which in

fact provides a full understanding of the net λ variation under uniaxial pressure. Namely, the a (c) reduction results in an increase (decrease) of the band width as expected, which enhances (suppresses) T_c . The increase of the band width results in a suppression of U/W , hence the electron correlation effect. This reduces the pairing interaction, while the self-energy correction due to the spin fluctuations is reduced at the same time. The former has an effect of enhancing T_c , while the latter suppresses superconductivity. In the case of Hg compound, the latter effect supersedes the former, resulting in an enhanced T_c .

It should be noted that the contribution from $r_{x^2-y^2}$, while relatively small for uniaxial compression, enhances T_c for *both* of the a - and c - axis compressions in marked contrast with the contributions from ΔE and W . This will become important in our analysis for hydrostatic pressures below.

IV. CALCULATION RESULTS: HYDROSTATIC PRESSURE

A. La_2CuO_4

Having identified the ingredients that determine the T_c variation against uniaxial pressures, let us now move on to *hydrostatic* compression. Here we optimize the lattice structure at a fixed unit cell volume $V (< V_0)$ by varying Poisson’s ratio, which we fit to the Burch-Marnaghan equation to obtain the most stable E_{tot} . Notably enough, for hydrostatic pressures λ in Fig.4 increases with the volume compression in *both* materials. This result qualitatively agrees with experimental results^{12,13}. To understand its mechanism, we can, as done above for uniaxial pressures, decompose the pressure effect on λ into the contributions from ΔE , W , and $r_{x^2-y^2}$ (arrows in Fig. 4(a)(b)). We can then realize that the variation of ΔE against hydrostatic pressure is not as straightforward as in uniaxial pressures. Namely, we can look

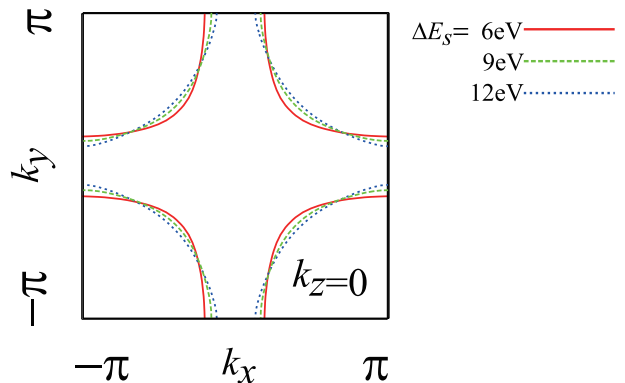


FIG. 3: The Fermi surface of the three-orbital model of the Hg cuprate for values of ΔE_s hypothetical varied from 6eV (nearly original value) to 12eV.

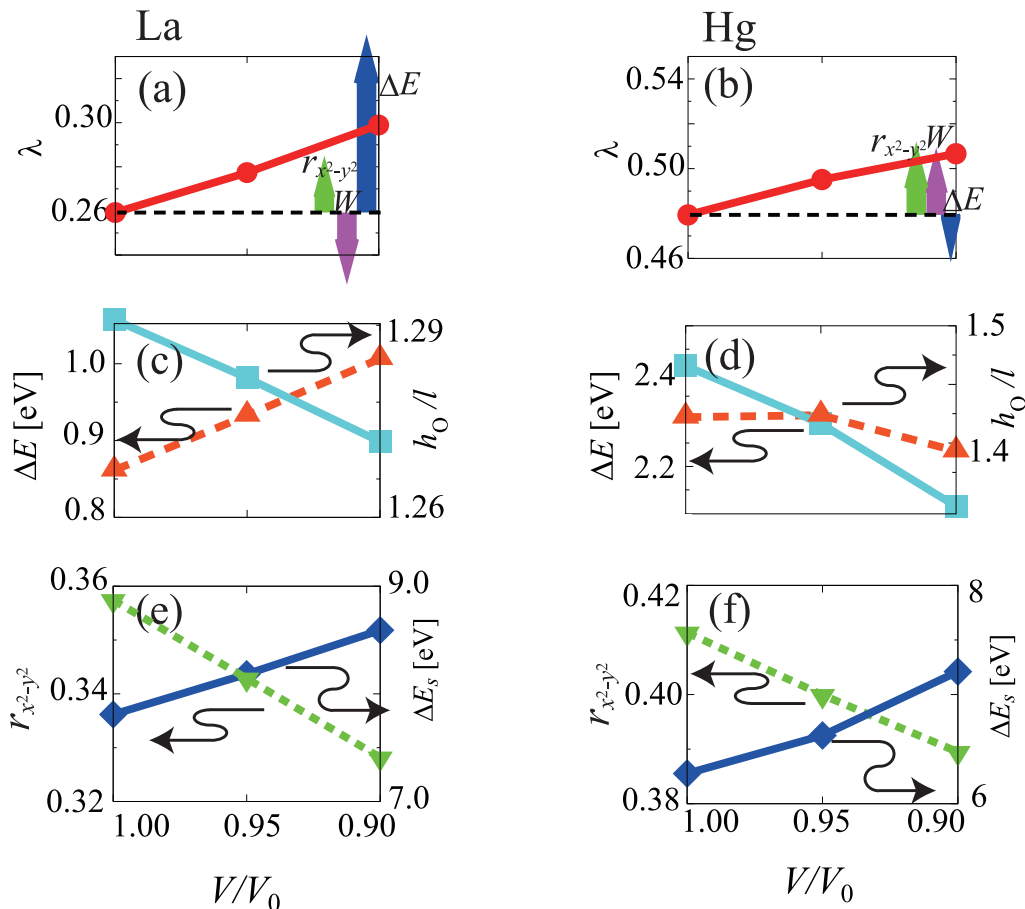


FIG. 4: For hydrostatic pressure applied to La(Hg) cuprates in the left(right) column, (a),(b): The eigenvalue λ of the Eliashberg equation plotted against the volume compression V/V_0 . Arrows are as in Fig.2 for $V/V_0 = 0.90$. (c),(d): the value of h_O/l (squares) and ΔE (triangles). (e),(f): the value of $r_{x^2-y^2}$ (triangles) and the $\Delta E_s \equiv E_{Cu4s} - E_{Cu3d_{x^2-y^2}}$ (diamonds). Lines are guide for the eye.

at ΔE along with the “aspect ratio” h_O/l against the volume reduction in Fig.4(c)(d), where h_O is the apical oxygen height and l the in-plane Cu-O distance. Under hydrostatic pressure, h_O/l decreases in both materials because of the larger compressibility along the c direction. One might then expect that this would reduce the crystal field splitting and hence ΔE , but actually this is by no means always the case. In fact, ΔE increases with pressure for La, which is because the Cu-O distance decreases, resulting in a larger crystal-field effect. Thus the T_c enhancement in La mainly comes from the increase of ΔE .

B. HgBa₂CuO₄

The above argument for La does not directly apply to Hg, since the original apical-oxygen height is larger, so that there is more room for the CuO octahedron to shrink along the c -axis than in La. Therefore, the h_O/l reduction is larger, resulting in a nearly constant ΔE against the decrease of V/V_0 . This further makes ΔE irrelevant

to the T_c variation in Hg under hydrostatic pressures. As seen in Fig.4 with arrows, main contributions to the T_c enhancement come from W and $r_{x^2-y^2}$, with similar magnitudes. As shown in Fig.4(e)(f), the decrease of $r_{x^2-y^2}$ originally comes from an increase of the level offset ΔE_s introduced above. The relatively large enhancement of the Cu4s level under hydrostatic pressure can be understood from Fig.1 (right), where all the ligands approaching Cu push up the energy level of the extended and isotropic Cu4s orbital to a larger extent than for the localized and anisotropic Cu3d orbitals. Thus a message here is the *hydrostatic and uniaxial pressures exert significantly different effects*. Specifically, the importance of $r_{x^2-y^2}$ becomes prominent in Hg in hydrostatic pressure because the $r_{x^2-y^2}$ -contribution is positive for both of a - and c -axis compressions, while W -contribution has opposite effects as shown in Fig.2.

As for the band-width effect, we have found here that Hg exhibits an effect opposite to La for the present electron-electron interaction strength. To elaborate this, we have performed a FLEX calculation for various interaction strengths over $6 < U/t < 10$, and found that

increasing the band width always results in an enhanced λ in Hg within the considered compression range, while in La a similar effect is obtained only for $8 < (U/t)$, with the effect reversing for smaller U . We have further noticed that this “sign change” in the band-width effect against U is peculiar to the systems having smaller ΔE . At any rate, the band-width effect is much smaller than the effect of ΔE in La, so that the effect of pressure-dependence of U does not affect the present conclusion.

C. Order of magnitude of dT_c/dP

Let us finally comment on the relation between the λ variation for hydrostatic pressures and the T_c enhancement in the actual pressure experiments. To see this, we have extended our calculation to lower temperatures for Hg, where λ becomes closer to unity (i.e., T approaches T_c). We find $\lambda \simeq 0.86$ at $T = 0.01$ eV for $V = 0.9V_0$, and the same value of λ attained at $T = 0.0088$ eV for $V = V_0$, so the temperature difference (a rough estimate of ΔT_c) amounts to $\simeq 14$ K. Since the compressibility is ~ 0.01 GPa $^{-1}$ ³⁵, this implies $dT_c/dP \sim 1$ K/GPa, which has the same order of magnitude found experimentally¹⁴.

V. CONCLUDING REMARKS

To summarize, we have identified the parameters that govern the T_c variation of the single-layered cuprates under pressure. For lower- T_c materials with small ΔE as exemplified by La₂CuO₄, T_c is sensitive to ΔE , which is identified to be the main contribution. For higher- T_c materials with large ΔE as exemplified by HgBa₂CuO₄, T_c is rather insensitive to ΔE , and important contribu-

tions are revealed to come instead from the Fermi surface roundness governed by the Cu4s orbital as well as the variation of the band width W . These effects coming from the electronic structure in the multi-orbital systems can be unified into a single picture in which the orbital distillation of the main band results in a higher T_c .

The present study can also shed light on a materials-science avenue for optimizing T_c . The strategy for enhancing T_c , as conceived here, is: (1) keep the level offset between the $d_{x^2-y^2}$ and d_{z^2} orbitals large (ideally, larger than U as shown in Fig.1 left), (2) expand the level offset between the Cu4s and the Cu3 $d_{x^2-y^2}$ as much as possible — this makes the Fermi surface more nested (fig.1 right), and (3) tune the band width W to a moderate value. In this sense, it is important to keep the distance h_O between apical oxygen and Cu atom, and it is also important to decrease the in-plane Cu-O bond length l . In other words, the desired situation for optimizing T_c should have an $a - b$ biaxial chemical pressure which reduces the length l from those in existing compounds, with the value of h_O kept high. This may be coupled to the possibility of the level offset ΔE_s controlled independently of ΔE by tuning length l ¹⁰.

VI. ACKNOWLEDGMENTS

The numerical calculations were performed at the Supercomputer Center, ISSP, University of Tokyo. This study has been supported by Grants-in-Aid for Scientific Research from JSPS (Grants No. 23340095, RA; No. 23009446, HS; No. 21008306, HU; and No. 22340093, KK and HA). RA acknowledges financial support from JST-PRESTO. DJS acknowledges support from the Center for Nanophase Material Science at Oak Ridge National Laboratory.

-
- ¹ J.D. Jorgensen, D.G. Hinks, O.Chmaissem, D.N. Argyiou, J.F. Mitchell, and B. Dabrowski, in *Lecture Notes in Physics*, **475**, p.1 (1996).
- ² A. Bianconi, G. Bianconi, S. Caprara, D. Di Castro, H. Oyanagi and N. L. Saini, *J. Phys.: Condens. Matter* **12**, 10655 (2000); A. Bianconi, S. Agrestini, G. Bianconi, D. Di Castro, and N. L. Saini, *J. Alloys Compd.* **317-318**, 537 (2001); N. Poccia, A. Ricci and A. Bianconi, *Adv. Condens. Matter Phys.* **2010**, 261849 (2010).
- ³ S. Maekawa, J. Inoue and T. Tohyama, in *The Physics and Chemistry of Oxide Superconductors*, edited by Y. Iye and H. Yasuoka (Springer, Berlin, 1992), Vol. **60**, pp. 105-115.
- ⁴ O.K. Andersen, A.I. Liechtenstein, O. Jepsen, and F. Paulsen, *J. Phys. Chem. Solids* **56**, 1573 (1995).
- ⁵ L.F. Feiner, J.H. Jefferson and R. Raimondi, *Phys. Rev. Lett.* **76**, 4939 (1996).
- ⁶ E. Pavarini, I. Dasgupta, T. Saha-Dasgupta, O. Jepsen, and O. K. Andersen, *Phys. Rev. Lett.* **87**, 047003 (2001).
- ⁷ C. Weber, K. Haule, and G. Kotliar, *Phys. Rev. B* **82**, 125107(2010).
- ⁸ C. Weber, C. -H. Yee, K. Haule and G. Kotliar, arXiv:1108.3028.
- ⁹ T. Takimoto, T. Hotta and K. Ueda, *Phys. Rev. B* **69**, 104504 (2004).
- ¹⁰ H. Sakakibara, H. Usui, K. Kuroki, R. Arita, and H. Aoki, *Phys. Rev. Lett.* **105**, 057003 (2010).
- ¹¹ H. Sakakibara, H. Usui, K. Kuroki, R. Arita and H. Aoki, *Phys. Rev. B* **85**, 064501 (2012).
- ¹² A.-K. Klehe, A. K. Gangopadhyay, J. Diederichs and J. S. Schilling *Physica* **213C**, 266 (1993); **223C** 121(1994).
- ¹³ L. Gao, Y. Y. Xue, F. Chen, Q. Xiong, R. L. Meng, D. Ramirez, C. W. Chu, J.H Eggert, and H.K. Mao, *Phys. Rev. B* **50**, 4260 (1994).
- ¹⁴ F. Hardy, N. J. Hillier, C. Meingast, D. Colson, Y. Li, N. Barisic, G. Yu, X. Zhao, M. Greven, and J. S. Schilling, *Phys. Rev. Lett.* **105**, 167002 (2010).
- ¹⁵ F. Gugenberger, C. Meingast, G.Roth, K. Grube, V. Breit, T. Weber, H. Wuhl, S. Uchida, and Y. Nakamura, *Phys. Rev. B* **49**, 13137 (1994).
- ¹⁶ C. Meingast, A. Junod and E. Walker, *Physica C* **272**, 106 (1996).
- ¹⁷ K. Shiraishi, A. Oshiyama, N. Shima, T. Nakayama and

- H. Kamimura, Solid State Commun. **66**, 629-632 (1988).
- ¹⁸ H. Kamimura and M. Eto, J. Phys. Soc. Jpn. **59**, 3053 (1990); M. Eto and H. Kamimura, J. Phys. Soc. Jpn. **60**, 2311 (1991).
- ¹⁹ A.J. Freeman and J. Yu, Physica B **150**, 50 (1988).
- ²⁰ X. Wang, H.T. Dang, and A. J.Millis, Phys. Rev. B **84**, 014530(2011).
- ²¹ L. Hozoi, L. Siurakshina, P. Fulde and J. van den Brink, Sci. Rep. **1**, 65 (2011).
- ²² S. Uebelacker and C. Honerkamp, Phys. Rev. B **85**, 155122 (2012).
- ²³ M. Mori, G. Khaliullin, T. Tohyama, and S. Maekawa, Phys. Rev. Lett. **101**, 247003 (2008)
- ²⁴ P. Blaha, K. Schwarz, G.K.H. Madsen, D. Kvasnicka, and J. Luitz, *Wien2k: An Augmented Plane Wave + Local Orbitals Program for Calculating Crystal Properties* (Vienna University of Technology, Wien, 2001).
- ²⁵ N. Marzari and D. Vanderbilt, Phys. Rev. B **56**, 12847 (1997); I. Souza, N. Marzari and D. Vanderbilt, Phys. Rev. B **65**, 035109 (2001). The Wannier functions are generated by the code developed by A. A. Mostofi, J. R. Yates, N. Marzari, I. Souza, and D. Vanderbilt, (<http://www.wannier.org/>).
- ²⁶ J. Kunes, R. Arita, P. Wissgott, A. Toschi, H. Ikeda, and K. Held, Comp. Phys. Commun. **181**, 1888 (2010).
- ²⁷ N.E. Bickers, D.J. Scalapino, and S.R. White, Phys. Rev. Lett. **62**, 961 (1989).
- ²⁸ T. Dahm and L. Tewordt, Phys. Rev. Lett. **74**, 793 (1995).
- ²⁹ K. Yada and H. Kontani, J. Phys. Soc. Jpn. **74**, 2161 (2005).
- ³⁰ H. Eisaki, N. Kaneko, D. L. Feng, A. Damascelli, P. K. Mang, K. M. Shen, Z.-X. Shen, and M. Greven, Phys. Rev. B **69**, 064512(2004).
- ³¹ F. Birch, Phys. Rev. B **71**, 809(1947).
- ³² J. D. Jorgensen, H. -B. Schuttler, D. G. Hinks, D. W. Capone, K. Zhang, and M. B. Brodsky and D. J. Scalapino, Phys. Rev. Lett. **58**, 1024 (1987).
- ³³ J.L. Wagner, P.G. Radaelli, D.G. Hinks, J.D. Jorgensen, J.F. Mitchell, B. Dabrowski, G.S. Knapp, M.A. Beno, Physica C **210**, 447 (1993).
- ³⁴ H. Takahashi, H. Shaked, B. A. Hunter, P. G. Radaelli, R. L. Hitterman, D. G. Hinks, and J. D. Jorgensen , Phys. Rev. B **50**, 3221 (1994).
- ³⁵ A. M. Balagurov, D. V. Sheptyakov, V. L. Aksenov, E. V. Antipov, S. N. Putilin, P. G. Radaelli and M. Marezio, Phys. Rev. B **59**, 7209 (1999).
- ³⁶ For a review, see D.J. Scalapino in *Handbook of High Temperature Superconductivity*, Chapter 13, Eds. J.R. Schrieffer and J.S. Brooks (Springer, New York, 2007).
- ³⁷ Th. Maier, M. Jarrell, Th. Pruschke, and J. Keller, Phys. Rev. Lett. **85**, 1524 (2000).
- ³⁸ P. R. C. Kent, T. Saha-Dasgupta, O. Jepsen, O. K. Andersen, A. Macridin, T. A. Maier, M. Jarrell, and T. C. Schulthess, Phys. Rev. B **78**, 035132 (2008).